Intercomparison of Satellite Precipitation with Gauge Data Using Point Frequency Analysis

Ozcan, Orkan and Musaoglu, Nebiye

Abstract: ***Climate has a dynamic structure denoting perpetual variability in temporal and spatial scales. Depending on space and time, rainfall amount has the most variation of the components of the climate system. In this study, the remote sensing dataset Tropical Rainfall Measurement Mission (TRMM) product at the 3-hour time scale has been validated with daily rain gauge measurements in order to characterize rainfall variability and to evaluate satellite rain estimates for agricultural and hydrological applications in the Southeastern Anatolia region. The precipitation retrievals from the TRMM satellite were compared with data from seven surface rain gauges within the period of 1998-2012. Spatiotemporal patterns through statistical analyses and regional frequency relationship were identified by fitting Generalized Extreme Value (GEV) rainfall distribution to the rainfall time series, and the fitting results were analyzed focusing on the behaviour of the shape parameter. In addition, spatial patterns and correlations of rainfall events across the study area were also analyzed by the calculation of the 90th, 95th and 99th percentiles. Furthermore, the recurrence intervals of large rainstorms have been identified for the rain gauge stations with the associated TRMM grid time series and spatial patterns in the study area have been evaluated. Thematic maps of the appropriate distribution function parameters were produced by performing the spatial evaluations of the designated regions with pixel-based point frequency analysis. Results indicate that there exist large discrepancies between rain gauge and TRMM data at mean rainfall values; however, least squares fits indicate reliable and quite linear correlation for the 90th, 95th and 99th percentiles (r^2=0.70, 0.77 and 0.75 respectively) and the annual maximum daily amount of precipitation (r^2=0.69). Recurrence intervals derived from rain gauge measurements for 10 to 40-year periods and a moving-window of 14-year intervals yielded similar results. Ultimately, the spatiotemporal pattern analysis of the computed extreme statistics is conducted using geographic information systems. Although rainfalls from each TRMM 3B42 grid cell are generally overestimated compared against rain gauge data, data compare well for stations that were located at approximately the mean elevation of the related TRMM 3B42 grids. The validated products can also be used as a framework for predicting the impact of hydrologic events in this area.***

Index Terms: ***Frequency Analysis, TRMM, GEV, Extreme Value Theory, Spatial Analysis.***

1. *Introduction*

EXTREME climatic events, such as heavy rainfall, floods and droughts, associated with both natural and human in nature, are being observed in recent years all over the world [1-4]. Increases in extreme events can have severe impacts on society and economy. Although hydrological extreme events occur randomly in time and space, their occurrences are generally regional phenomena by nature that exhibit a certain degree of areal-wide similarity and continuity. Existing approaches to estimating the recurrence intervals of extreme events are mainly based on statistical analyses of long-term observational data. Therefore, frequency analysis, which constitutes a theoretical basis for the understanding of hydrological processes, is of considerable importance for coping with heavy rainfall events and resulting floods [5-9].

The interest in studying these extreme natural events is to alleviate their impact on humans, properties and sources of income such as agricultural fields. Extreme value theory has long been applied to the study of these infrequent events and has been proven to be reliable in fitting models to historical data. The application of the extreme value theory has been used extensively in diverse fields such as in finance, environmental studies, economics, hydrology and climatology [10, 11]. Extreme value distributions are the limiting distributions for the minimum or the maximum of a very large collection of random observations from the same arbitrary distribution. The knowledge of the variation of rainfall

Manuscript received April 18, 2017.

O. Ozcan is with the Eurasia Institute of Earth Sciences, Istanbul Technical University, Maslak, Istanbul, 34469, TURKEY (phone: +90212-285-6108; fax: +90212-285-6210; e-mail: ozcanork@itu.edu.tr). (Corresponding author).

N. Musaoglu is with the Geomatics Engineering Department, Istanbul Technical University, Maslak, Istanbul, 34469, TURKEY (e-mail: musaoglune@itu.edu.tr).

distribution in the hydrological cycle has a great importance in order to understand and to predict climate change and weather anomalies.

Hydrologic frequency analysis is usually performed based on the appropriate probability distribution, which is selected based on statistical tests for extreme hydrologic data collected in a specific region [12]. A number of frequency distribution models have been used in the past for hydrologic frequency determination. Though several probability models have been developed to describe the frequency distribution of extreme hydrologic events, major problems arise when selecting the best method to use. The reason for that is the fact that there is no general agreement as to which distribution, or distributions should be used for the frequency analysis of extreme hydrologic events. Therefore, the selection of an appropriate model depends mainly on the characteristics of available data at the particular site [13].

Regionalization of hydrologic processes takes advantage of and utilizes the similarities in extreme hydrologic events by pooling data from different sites to enhance estimation reliability and/or to transfer information from gauged sites to ungauged locations where the data information is needed but unavailable. Point measurements of precipitation serve as the primary data source for territorial analysis. However, even the best measurement of precipitation at one point is only representative of a limited area. The spatial and temporal variability of precipitation, along with surface characteristics and topography, are of paramount importance in understanding hydrological processes and land-atmosphere interactions over semi-arid and arid regions. In semi-arid to arid regions, landscape-shaping hydrologic events are often associated with extreme rainfall or flooding events [4, 14-16]. The spatiotemporal structure of precipitation greatly affects land surface hydrological fluxes and states [17, 18]. With the purpose to obtain estimates that are more accurate and a wider areal coverage of precipitation, satellite-based rainfall sensors with various spatial scales and resolutions have been deployed over the last decades [19, 20].

The Tropical Rainfall Measuring Mission (TRMM) which is a unique platform used with the aim of characterizing tropical rainfall with remote sensors from space, has provided rain radar and microwave radiometric combined data with a precipitation radar (PR) and a TRMM microwave imager (TMI) radiometer [21] since 1997. The product 3B42 merges TRMM satellite observation with other passive microwave radiometers that measures the vertical distribution of precipitation between the latitudes ± 50° with providing sampling of the complete diurnal cycle of rainfall. Several studies suggest that the TRMM product 3B42 surface-rainfall rate is comparable to the other surface observation [22-24], although the spatial scale of the rainfall data makes direct comparison to gauge data difficult [2].

Rain gauges and other ground-based instruments play a key role in both constructing and validating remote-sensing based rainfall estimates [25]. Some global and regional validations have been reported for different satellite rain products [26-29]. In addition, a number of efforts have been made to compare TRMM products with other measurements [30-33], but these studies have usually been limited to comparisons on a monthly scale. In southeastern region of Turkey, where remotely sensed information is needed most, there has been very little validation work.

Extreme-value theory is often required to find return values for recurrence intervals that amply exceed the record length. In environmental sciences, using specific thresholds such as the 90^{th}, 95^{th} and 99^{th} percentiles of precipitation days or block maxima with Generalized Extreme Value (GEV) distribution approach to define extreme events, can help decision makers determine the maximum level of risk against which they should protect [34]. The GEV distribution is a family of continuous probability distributions developed within extreme value theory, which is a robust framework to analyze the tail behaviour of distributions. Accurately estimating the tails of distributions is also important for many risk-based applications.

In the present study, 15 years (1998–2012) of TRMM product 3B42 was validated and compared with 7 rainfall gauges (entire length 43 years, from 1970 to 2012) in order to characterize the rainfall variability in a part of semi-arid South-eastern Anatolia region.

Daily rainfall amounts of extreme events have been determined by the calculation of the 90^{th}, 95^{th} and 99^{th} percentiles of the distribution for days with precipitation. The recurrence intervals for different years have been estimated using GEV distribution of annual maximum daily rainfall amounts and described how they vary among the rain gauge stations and the TRMM 3B42 grid cells. Besides, spatiotemporal patterns through statistical analyses were identified by fitting GEV rainfall distribution to the rainfall time series, and the fitting results were analyzed focusing on the behaviour of the shape parameter for both rain gauge stations and the associated TRMM 3B42 grid cells.

2. *Study Area and Data Structure*

The Southeastern Anatolia Region is under the

influence of both the continental climate and the Mediterranean climate. The long summers are hot and dry. The winters are cold with rainfall and snowfall. The annual average temperature is 18 °C and annual rainfall is around 350 mm. There is significant seasonal variation in precipitation. Rainfall is highly seasonal with more than 80% concentrated in the period November through March. The area receives almost no rain during the summer at which time irrigation becomes crucial. The mean annual rainfall rates have been decreased significantly for the past 42 years; however, summer rainfall series indicate a significant upward trend in this region. Increased rainfall amounts, with flush flooding, may have led soil erosion to be more disastrous in this semi-arid region with sparse vegetation cover.

In recent years, some changes have been experienced in the climate in the region related to the dam construction and lake formation within the scope of the Southeastern Anatolia Project (GAP) (Fig. 1). The research region has a higher variability in crop yield and studies showed that the rainfall had a very significant impact on agricultural production in the region [35]. Daily rainfall data for each station have been compared to the associated TRMM 3B42 grid cells [22]. The TRMM data come in a gridded format with a spatial resolution of 0.25° x 0.25° (~30 km x 30 km) and with a temporal resolution of 3 hours. For all spatiotemporal analyses, daily rainfall amounts have been used as integrated from the 3-h data.

3. METHODOLOGY

The first purpose of the study is to collect the field data sources such as historic climate and hydrologic data in order to identify the extreme events. To find the most appropriate distribution(s) for describing the annual maxima of daily variable, GEV (Generalized Extreme Value), Gamma and EV (Extreme Value) distributions were compared by using different goodness of fit (GOF) criterion such as Chi-Squared (χ^2) and Kolmogorov-Smirnov (K-S) tests. Once a distribution function is assumed to be selected for study at hand, it remains to estimate its parameters from the sample data and to test the goodness of fit.

In regional frequency analysis [36], the final and important objective is to determine the robustness of the selected distribution in constructing reasonable and reliable estimation at all sites. The capabilities of the selected regional frequency distribution were further investigated for estimation of design variable quantiles of specific recurrence intervals and the variations among the stations and the associated TRMM 3B42 grid cells were described.

3.1. Distribution Functions

GEV distribution is built into the extreme value

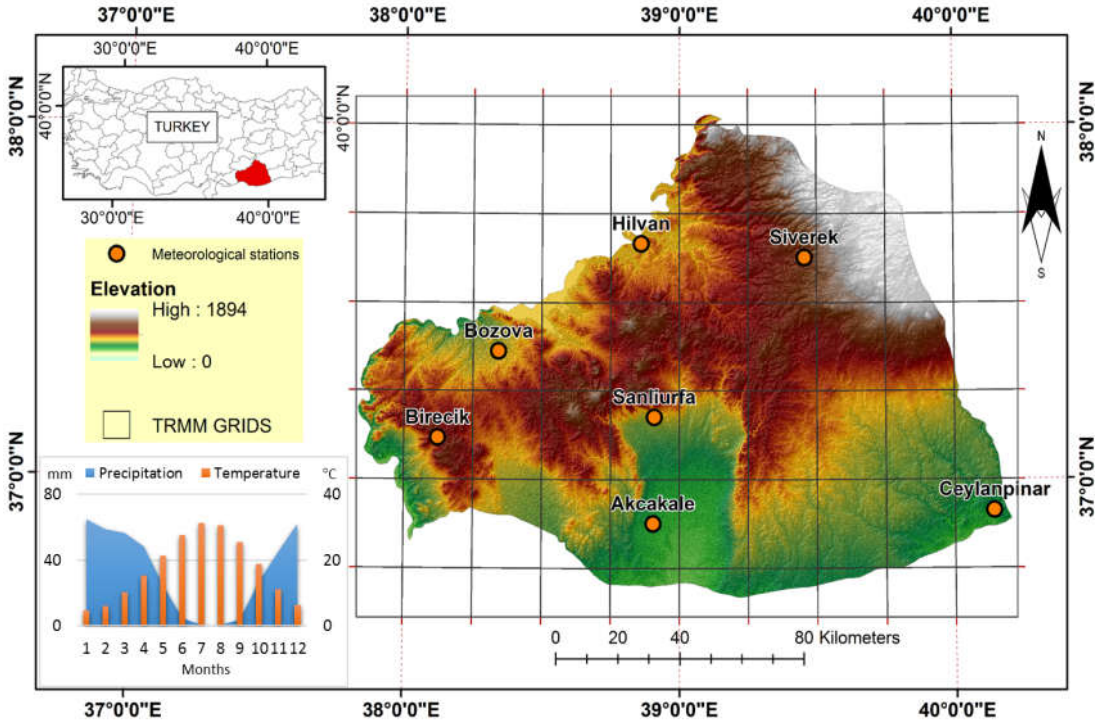

Fig 1: The locations of the rain gauge stations with associated TRMM grid cells. The inset graphic represents the monthly long-term mean rainfall and temperature variations of the entire rain gauge stations within the period of 1970 to 2012 in the study region.

theory to combine the Gumbel, Frechet, and Weibull distributions, known as the extreme value distribution types of I, II, and III.

On the GEV distribution, x is a random variable that only takes continuous real values. The probability density function (PDF) and the cumulative distribution function (CDF) of a GEV distribution are defined by Equations 1 and 2, respectively.

$$f(x)=\begin{cases}\frac{1}{\sigma}\left[1+\xi\left(\frac{x-\mu}{\sigma}\right)\right]^{\left(\frac{-1}{\xi}\right)-1}\exp\left\{-\left[1+\xi\left(\frac{x-\mu}{\sigma}\right)\right]^{\frac{-1}{\xi}}\right\} \\ where \xi\neq 0 \\ \frac{1}{\sigma}\exp\left\{\frac{x-\mu}{\sigma}\right\}\exp\left\{-\exp\left(\frac{x-\mu}{\sigma}\right)\right\} \\ where \xi=0\end{cases} \quad (1)$$

$$F(x:\mu.\sigma.\xi)=\exp\left\{-\left[1+\xi\left(\frac{x-\mu}{\sigma}\right)\right]^{\frac{-1}{\xi}}\right\} \quad (2)$$

where $1+\xi(x-\mu)/\sigma>0$,

In a GEV distribution, there are three model parameters: the location parameter μ, the scale parameter σ, and the shape parameter ξ. The location parameter (μ) describes the shift of a distribution in a given direction on the horizontal axis; the scale parameter (α) describes how spread out the distribution is, and defines where the bulk of the distribution lies. As the scale parameter increases, the distribution will become more spread out. Shape parameter determines the behaviour of the tail of the distribution and in general, improves the fit to the upper tail (i.e., extremely large values). The shape parameter is derived from skewness, as it represents where the majority of the data lies, which creates the tail(s) of the distribution. Distribution type is defined with $\xi=0$, $\xi>0$, and $\xi<0$ and can be likened to the Gumbel, Frechet, and Weibull distribution. In this study, GEV distribution parameters have been estimated by using Maximum Likelihood Estimation (MLE) at 5% level of significance. Assuming the data stationary, the annual maximum daily rainfalls at different return periods can be estimated using the inverse cumulative distribution function of the GEV distribution

The PDF and CDF of Gamma distribution having shape (*α*), which allows a distribution to take on a variety of shapes, and scale (*β*) parameters which stretch/squeeze the pdf function, are given in Equations 3 and 4.

$$f(x:\alpha.\beta)=\frac{x^{\alpha-1}}{\beta^{\alpha}\Gamma(\alpha)}\exp[-x/\beta] \quad (3)$$

where $x>0,\alpha,\beta>0$,

$$F(x)=\frac{\Gamma(x/\beta)\alpha}{\Gamma(\alpha)} \quad (4)$$

where $\Gamma(x)$ is incomplete Gamma function. The PDF and CDF of EV distribution having location (μ) and scale (*β*) parameters are given in Equations 5 and 6, respectively.

$$f(x)=\frac{1}{\beta}\exp\left(\frac{x-\mu}{\beta}\right)\exp\left[-\exp\left(\frac{x-\mu}{\beta}\right)\right] \quad (5)$$

$$F(x)=\exp\left[-\exp\left(\frac{x-\mu}{\beta}\right)\right] \quad (6)$$

The shape parameter governs the shape of the rainfall distribution and the scale parameter determines the variation of rainfall series that is given in the same unit as the random variable χ.

Maximum annual and daily rainfalls from

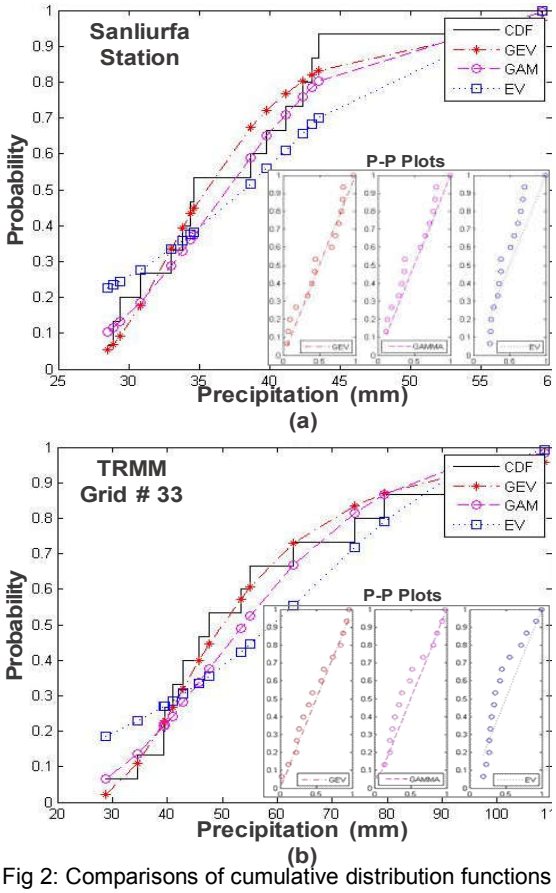

Fig 2: Comparisons of cumulative distribution functions (CDFs) for (a) Sanliurfa station and (b) the related TRMM grid. The inset graphics represent the probability-probability (P-P) plots of each distribution function.

TRMM 3B42 dataset were calculated based on the daily measurement intervals over the time period from 1998 to 2012. The performance of the distribution functions has been investigated by CDF and probability-probability (P-P) plots (Fig. 2).

The P-P plot, which is a graph of the empirical CDF values plotted against the theoretical (fitted) CDF values, was used to determine the goodness of fit. Figure 2 shows an example of comparisons of CDFs for Sanliurfa Station and the related TRMM grid. In order to remove any spatial inconsistencies regarding the precision of the observed data related to recording of the trace values, all wet days for each grid of TRMM (rainfall <0.1mm/day) were extracted. The rainfall statistics were calculated by fitting GEV, Gamma, and EV with comparing these datasets to the available station data established on the study region for the same periods.

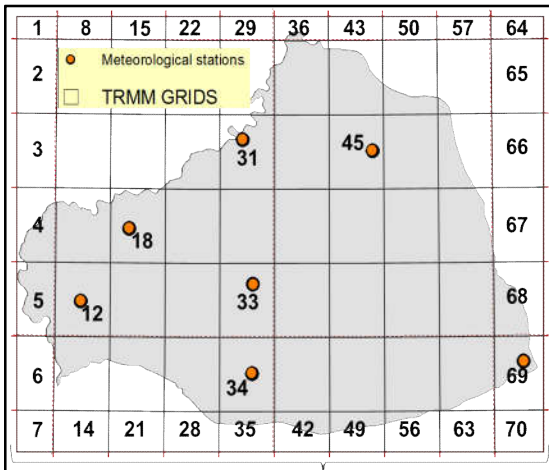

TRMM-Daily Data			GRID #		
DATA	Dist. Func.	Parameters	1	....	70
WET DAYS (>0.1 mm/day)	GEV	Shape, ξ	0,638	....	0,978
		Scale, σ	1,852	....	2,579
		Location, μ	1,891	....	2,117
	GAMMA	Shape, α	0,961	....	0,706
		Scale, β	5,110	....	11,707
	EV	Location, μ	9,376	....	16,096
		Scale, β	16,151	....	27,240

Fig 3: Parameter estimation of the distribution functions of TRMM grids by using Maximum Likelihood Estimation (MLE) at 5% level of significance.

Examples of parameter derivation from the TRMM data for the three distributions are shown in Figure 3. In general, a distribution with a larger number of flexible parameters would be able to model the input data more accurately than a distribution with lower number of parameters [37].

3.2. Goodness of Fit (GOF) Tests

The goodness of fit involves identifying a distribution that fits the observed data. When computing the magnitudes of extreme events, such as excessive precipitation, it is required that the probability distribution function is invertible, so that a given value of recurrence interval and the corresponding value of frequency factor can be determined. In this study, Chi – Square (χ^2) test and a Kolmogorov–Smirnov (K–S) tests were performed to determine the goodness of fit (GOF) for the proposed distribution functions. The χ^2 test statistics were obtained by Equation (7) after calculating the sample frequency and the theoretical frequency for the specific probability distribution function.

$$x^2 = \sum_{i=1}^{k}\left(\frac{n_i - np_i}{np_i}\right)^2 \qquad (7)$$

where n is the number of sample data points and k is the number of class intervals. Therefore, n_i and np_i are the frequencies and theoretical frequencies in the i^{th} interval of sample data, respectively. p_i is the theoretical probability for the i^{th} interval of data. The value of χ^2 approaches χ^2 distribution with the degree of freedom $v = k - h - 1$ where h is the number of parameters. In this study, the χ^2 test was performed at a significance level of 5 %.

The K–S test statistics indicate the maximum deviation between the empirical distribution and the theoretical distribution, which is calculated using Equation (8).

$$D_{Max} = Max\left|F(x) - F_0(x)\right| \qquad (8)$$

where $F(x)$ is empirical distribution of the observed data, and $F_0(x)$ is theoretical distribution. If the value of D_{Max} is larger than the critical value D_n^x, then the null hypothesis is rejected. This test was performed in this study and P-values of this GOF statistics have been calculated for GEV, Gamma and EV distributions with a significance level of 5 % using MLE.

The performance of distributions has been investigated using χ^2 and K-S GOF tests and the maximum precipitation values for each year have been calculated from two different datasets. An example for a comparison of a station to related TRMM grid statistics is given in Figure 4. The values of GOF criteria were calculated and the best distribution was chosen based on the minimum error of GOF tests. The distributions were ranked in ascending order based on the obtained values. The results showed that the EV distribution performed poorly whereas GEV and GAMMA distributions provided good estimates for rainfall retrievals in the region. According to the test results, the GEV distribution could be

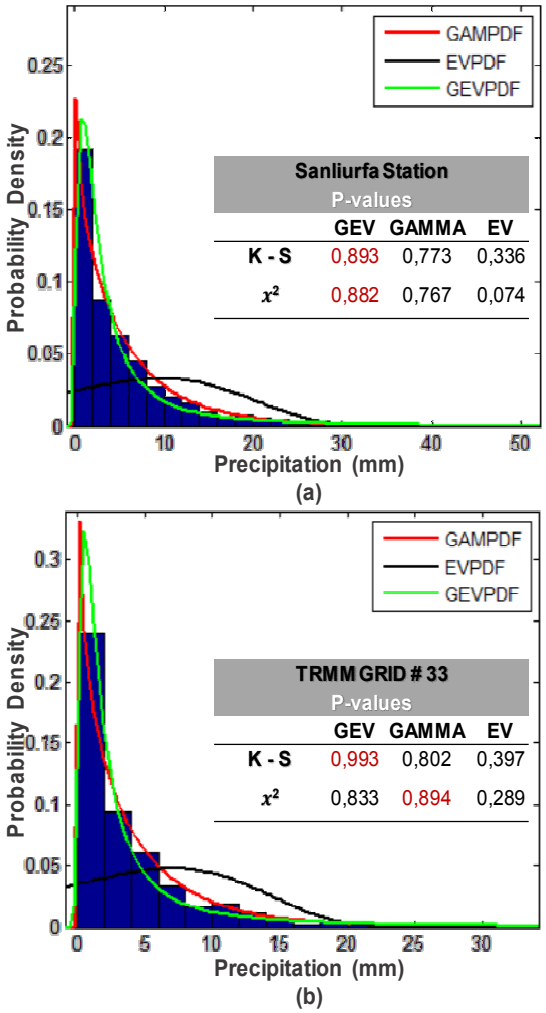

Fig 4: Comparisons of probability density functions (PDFs) for (a) Sanliurfa station and (b) the related TRMM grid. The inset tables represent the goodness of fit test results.

applied to most of the stations considered in this study.

3.3. Recurrence Intervals

One approach to define extreme precipitation events is to calculate recurrence intervals of the event based on the annual maximum daily rainfall series [1]. The recurrence interval, also called the return period, refers to the maximum value that is expected to be reached within the period of time *T* with period *p*, or in other words, in the *T* and *p* period, precipitation will reach the maximum value one time [36, 38].

In the study, GEV distribution was selected as regional frequency distribution depending on GOF test results for estimation of design variable quantiles of specific recurrence intervals. Then it was described how they vary among the stations and the associated TRMM 3B42 grid cells by using Equation (9). To acquire recurrence intervals, first a series of extreme values are obtained from the historical data set and the GEV CDF is calculated from this series.

This function contains shape, location, and scale parameters that are estimated based on the temporal length and distribution of values contained in the dataset. To fit values one can get the median and then vary μ until it fits the list of values. The observed time series of annual maximum daily rainfall at each gauge was plotted for 43 years along with their corresponding simulated rainfalls to illustrate the model ability to reproduce extremes. Figure 5 shows the comparisons of rainfall quantiles corresponding to return periods for Sanliurfa station based on different timescales and the related TRMM grid that is based on 1998–2012 timescale. When the station timescale is expanded to 1970 - 2012, the station curve significantly converges to the TRMM curve. Accordingly, comparison of gauge and TRMM based recurrence intervals has also been determined for different timescales.

$$R_p^T = \begin{cases} \mu - \dfrac{\sigma}{\xi}\left\{1 - \left[-\ln\left(1-\dfrac{1}{T}\right)\right]^{-\xi}\right\}, \xi \neq 0 \\ \mu - \sigma \ln\left\{\left(-\ln\left(1-\dfrac{1}{T}\right)\right)\right\}, \xi = 0 \end{cases} \quad (9)$$

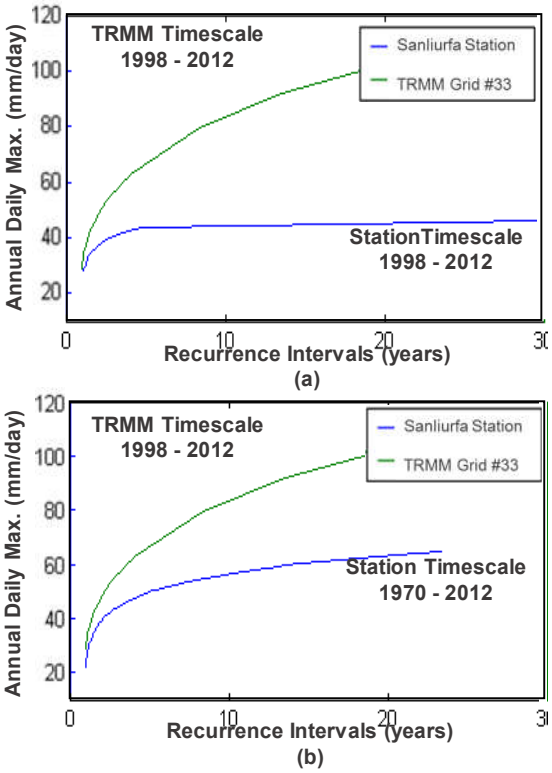

Fig 5: Comparisons of rainfall quantiles corresponding to return periods for Sanliurfa station based on (a) 1998-2012, (b) 1970-2012 timescale and the related TRMM grid (based on 1998–2012 timescale).

4. RESULTS AND DISCUSSION

The regional frequency relationship has been developed by fitting the best distribution function that was achieved by applying GOF tests. In the study, GEV distribution, which comprises the three limiting types as special cases for specific values of its shape parameter, yielded the optimal result. The largest daily rainfall values in each of n years, known as block maximum series, was chosen for the comparison of the return periods.

The annual maximum daily rainfall values associated with different return periods have been determined within the period of 1970 - 2012. Besides, comparison of gauge-based and TRMM-based recurrence intervals has been evaluated within 10 to 40-year periods and a moving-window of 14-year intervals (Figure 6). Recurrence intervals derived from rain-gauge measurements for 10 to 40-year periods and a moving-window of 14-year intervals yielded similar results at all stations. Nevertheless, the comparison of 15 years of precipitation retrievals from the TRMM satellite with data from seven surface rain gauge stations shows that the most remarkable result observed in Akcakale station that is located in the southernmost part of the study region.

In addition to the estimation of the recurrence intervals for different years, statistical evaluations also included the calculation of the 90th, 95th and 99th percentiles in the study area. Based on the chosen threshold of the percentiles, daily rainfall amounts of extreme events for all rain gauge stations were determined and compared with the related TRMM grid cells (Figure 7a). In the calculation of percentiles, all days with no precipitation or days with precipitation of less than 0.1 mm were ignored (i.e., we only considered wet days). Results indicate that there exist large discrepancies between rain gauge and TRMM data at mean rainfall values however, least squares fits indicated some high and quite linear correlation for the 90th, 95th, 99th percentiles (r^2=0.70, 0.77 and 0.75 respectively) and the annual maximum daily amount of precipitation (r^2=0.69).

The spatiotemporal pattern analysis of the computed extreme statistics is conducted using geographic information systems. The spatial distribution of extreme events defined by 90th percentile is shown in Figure 7b. Although rainfalls from each TRMM 3B42 grid cells are generally overestimated compared against rain gauge data, data compare well for stations that were located at approximately the mean elevation of the related TRMM 3B42 grid cell. In Figure 7c, the spatial distributions of the GEV shape parameter of rain gauges and TRMM 3B42 states that the increase in the shape parameter explains the differences between the changes in large quantiles of the daily precipitation extremes. Large positive shape parameter estimates can be a consequence of a few extremely high rainfall events and describes situations where extremes have an upper bound. Although there were similar results in shape values between the TRMM and rain gauge data in the northern (Siverek) and the southern (Akcakale) of the study area, some significant differences were encountered in the northwestern (Hilvan and Bozova) and the southeastern

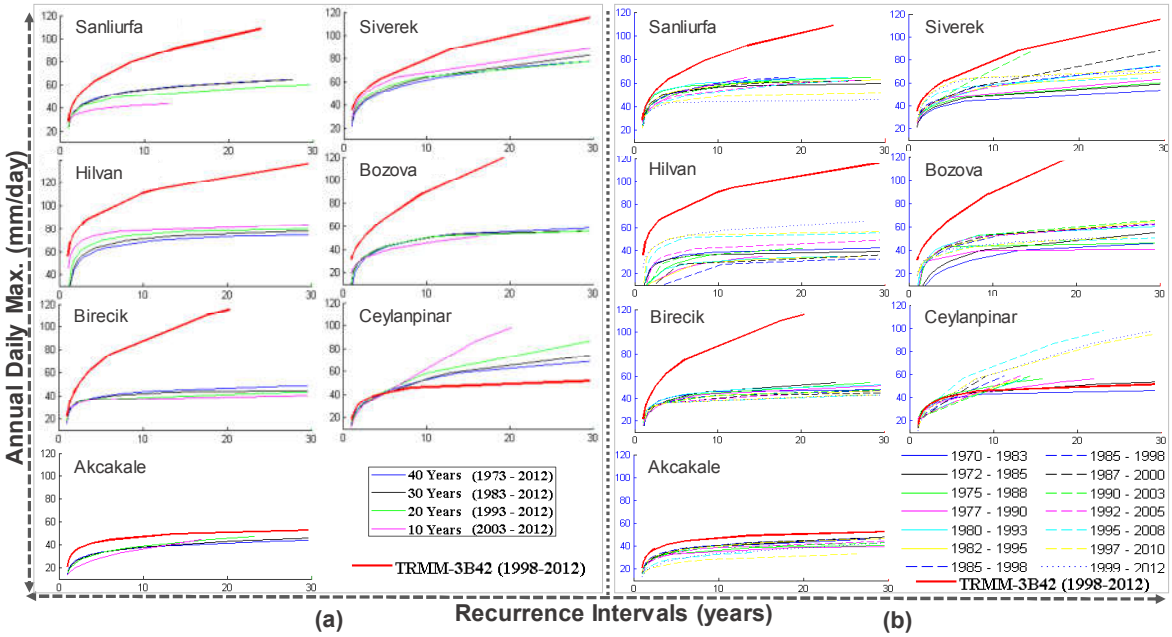

Fig 6: Comparison of gauge-based and TRMM-based recurrence intervals within (a) 10 to 40-year periods and (b) a moving-window of 14-year intervals.

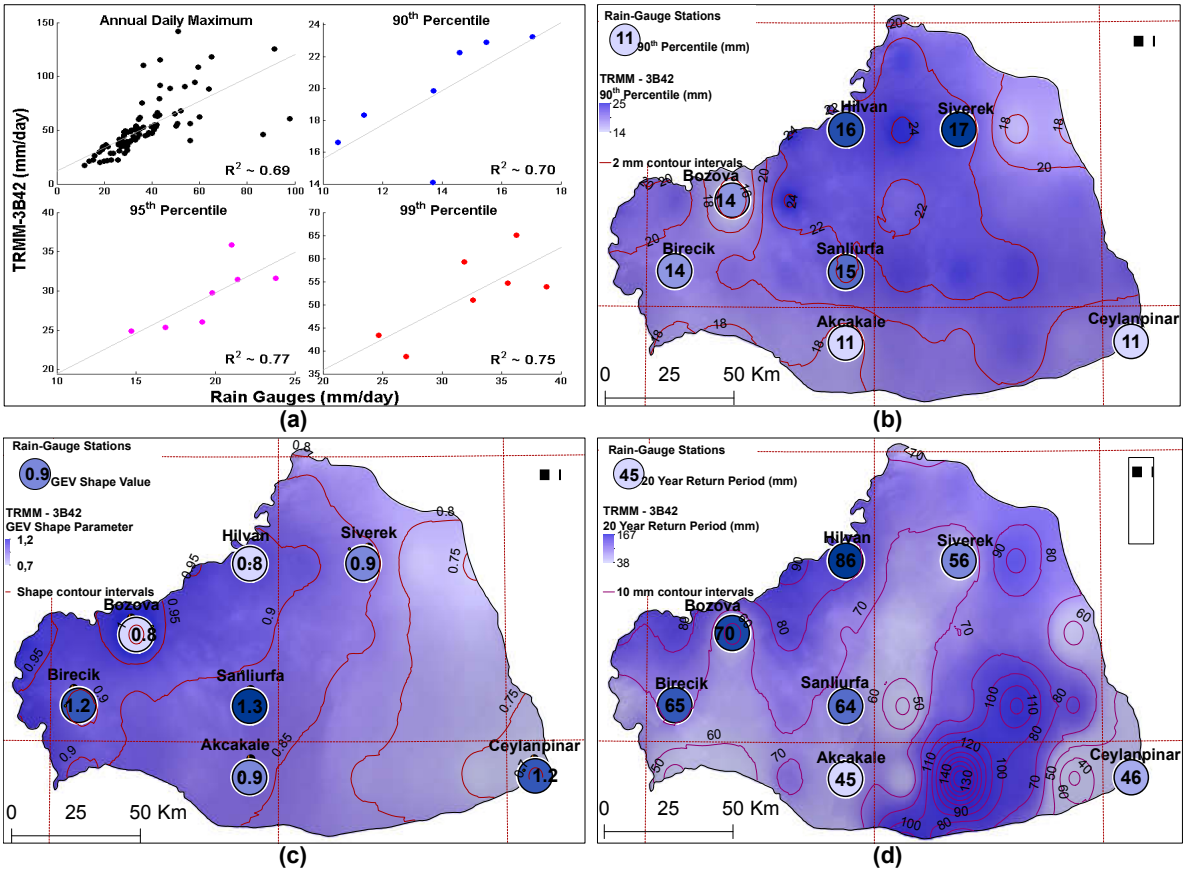

Fig 7: (a) Correlations of the annual daily maximum rainfalls and the 90th, 95th, 99th percentiles between rain gauges and TRMM 3B42 grid cells and spatial distributions of extreme events defined by (b) 90th percentile, (c) the GEV shape parameter, (d) 20-year recurrence intervals of rain gauges (in circles) and TRMM 3B42 for the period of 1998 to 2012. Coloured backgrounds show the result from Inverse Distance Weighted (IDW) interpolation and are based on TRMM values.

(Ceylanpinar) part of the study area. The comparison of the spatial distributions for the 20-year return period of extreme events is shown in Figure 7d. Values indicate maximum daily rainfall associated with 20-year recurrence intervals. The spatial gradient is based on an inverse-distance-weighted (IDW) interpolation algorithm and applied to 15-years of TRMM data. Similar results in recurrence intervals were obtained between the TRMM and rain gauge data for the entire region especially in the southern stations (Akcakale and Ceylanpinar).

Rainfall amounts between rain gauge and TRMM 3B42 data vary significantly. However, some statistical and spatial results are remarkable well correlated. We conclude that TRMM 3B42 can be used to assess first-order rainfall statistics and recurrence intervals. Ultimately, the validated products can be used as a framework for predicting the impact of hydrologic events in this area.

5. CONCLUSION

Since the purpose of the study is to validate and to analyze the spatiotemporal patterns of extreme precipitation events, the TRMM 3B42 product was compared with the rain gauge network in the study area. Accurate measurements of precipitation on a variety of space and time scales are important because it reflects the weather systems in the region and the characteristics of its meteorological and hydrological cycle. While rain gauge measurements are often used to tune hydrologic models, they are limited by their spatial coverage. Satellite rainfall estimates are being used widely in place of gauge observations or to supplement gauge observations since remote sensing techniques provide an excellent complement to continuous monitoring of precipitation events both spatially and temporally. Beside this, the historical record of precipitation observations is limited mostly to land areas where rain gauges can be deployed, and measurements from those instruments are sparse over large and meteorologically important regions of the Turkey, such as over the Southeastern Anatolia.

Identifying hydrometeorologic extreme events, planning for weather-related emergencies, both rely on knowledge of the frequency of hydroclimatic extreme events. In particular, erosion and removal of the fertile soil layer

through these extreme events is one of the most serious problems in semi-arid to arid regions, especially in Mediterranean climates. This kind of problems and their effects through time are keys in sustaining agriculture and socio-economic development, and adoption strategies must be carefully developed based on knowledge and observation.

ACKNOWLEDGMENT

The data used in this study were acquired as part of the Tropical Rainfall Measuring Mission (TRMM) sponsored by the Japan National Space Development Agency (NASDA) and the US National Aeronautics and Space Administration (NASA). The Turkish State Meteorological Service graciously provided rain gauge data.

REFERENCES

[1] Kunkel, K. E., Andsager, K., and Easterling D. R., "Long-term trends in extreme precipitation events over the conterminous US and Canada," J. Climate, 1999, 12, 2515–2527.

[2] Bookhagen, B., "Appearance of extreme monsoonal rainfall events and their impact on erosion in the Himalaya," Geomatics, Natural Hazards Risk, 2010, 1, 1, pp. 37-50.

[3] Zscheischler, J., Mahecha, D. M., Harmeling, S., Reichstein, M., "Detection and attribution of large spatiotemporal extreme events in Earth observation data," Eco. Inf., 2013, 15, 66-73.

[4] Boers, N., and co-authors., "Complex networks identify spatial patterns of extreme rainfall events of the South American Monsoon System," Geophys. Res. Lett., 2013, 40, 10.1002/grl.50681.

[5] Milly, P. C. D., J. Betancourt, M. Falkenmark, R. M. Hirsch, Z. W. Kundzewicz, D. P. Lettenmaier, and Stouffer R. J., "Stationarity is dead: whither water management?," Science, 2008, 319(5863), 573–574.

[6] IPCC, "Summary for policymakers. Climate Change 2014 : Impacts, adaptation, and vulnerability. Part A : Global and Sectoral Aspects. Contribution of Working Group II to the Fifth Assessment Report of the Intergovernmental Panel on Climate Change," *Cambridge University Press*, 2014, 1–32.

[7] Jiang, T., T. Fischer, X. X. Lu, and He, H. M., "Larger Asian rivers: Impacts from human activities and climate change," Quaternary International, 2015, 380–381, 1–4.

[8] Fischer, E. M., and Knutti, R., "Anthropogenic contribution to global occurrence of heavy-precipitation and high temperature extremes," Nature Climate Change, 2015, 5(6), 560– 564.

[9] Serinaldi, F., and Kilsby, C. G., "Stationarity is undead: uncertainty dominates the distribution of extremes," Advances in Water Resources, 2015, 77, 17–36.

[10] Jenkinson, A. F., "The frequency distribution of the annual maximum (or minimum) values of meteorological elements," Quarterly J. of the Royal Meteorological Society, 1955, 87, 158-171.

[11] Embrechts, P., Resnick, S., and Samorodnitsky, G., "Extreme value theory as a risk management tool," North American Actuarial Journal, 1999, 3, 30-41.

[12] Yoon, P., Kim, T. W., Yoo, C., "Rainfall frequency analysis using a mixed GEV distribution: a case study for annual maximum rainfalls in South Korea," Stoch Environ Res Risk Assess., 2013. doi: 10.1007/s00477-012-0650-5

[13] Olofintoye, O. O., Sule, B. F., Salami, A. W., "Best–fit Probability distribution model for peak daily rainfall of selected Cities in Nigeria," New York Science Journal, 2009, 2(3), 1-12.

[14] Bookhagen, B., Thiede, R. C., Strecker. M. R., "Abnormal Monsoon years and their control on erosion and sediment flux in the high, arid northwest Himalaya," Earth and Planetary Science Letters, 2005, 231, 131-146.

[15] Wulf, H., Bookhagen, B., and Scherler, D., "Climatic and Geologic Controls on Suspended Sediment Flux in the Sutlej River Valley, Western Himalaya," HESS, 2012, 16, 2193 - 2217.

[16] Wulf, H., Bookhagen, B., and Scherler, D., "Seasonal Precipitation Gradients and their Impacts on Fluvial Sediment Flux in the Northwest Himalaya," Geomorphology, 2010, 118, 13-21.

[17] Fekete, B. M., Vorosmarty, C. J., Roads, J. O., and Willmott C. J., "Uncertainties in precipitation and their impact on runoff estimates," J. Climate, 2003, 17, 294–304.

[18] Gottschalck, J., Meng, J., Rodell, M., and Houser, P., "Analysis of multiple precipitation products and preliminary assessment of their impact on Global Land Data Assimilation System land surface states," J. Hydrometeor., 2005, 6, 573–598.

[19] Ozcan, O., Bookhagen, B., Musaoglu, N., "Analyzing spatiotemporal patterns of extreme precipitation events in Southeastern Anatolia," International Archives of the Photogrammetry, Remote Sensing and Spatial Information Sciences, vol XL-7/W2, ISPRS2013-SSG, 11–17 November 2013, Antalya, Turkey, pp 195–200. doi:10.5194/isprsarchives-XL-7-W2-195-2013

[20] Katsanos, D., Retalis, A., Tymvios, F., Michaelides, S., "Analysis of precipitation extremes based on satellite (CHIRPS) and in situ dataset over Cyprus," Natural Hazards, 2016, 83, 53-63. DOI: 10.1007/s11069-016-2335-8

[21] Okamoto, K., "A short history of the TRMM precipitation radar, in Cloud Systems, Hurricanes, and the Tropical Rainfall Measuring Mission (TRMM)," *Meteorol. Soc., Boston, Mass,* Meteorol. Soc. Monogr., 2003, vol. 29, pp. 187–195, Am.

[22] Huffman, G. J., et al., "The TRMM Multisatellite Precipitation Analysis: quasi-global, multiyear, combined sensor precipitation estimates at fine scales," J. Hydromet, 2007, 8, 38–55.

[23] Koo, M. S., Hong, S. Y., and Kim, J., "An evaluation of the TRMM Multi-Satellite Precipitation Analysis (TMPA) data over South Korea," Asia-Pacific J. of Atmos. Sci., 2009, 45, 265–282.

[24] Sapiano, M. R. P., and Arkin, P. A., "An intercomparison and validation of high resolution satellite precipitation estimates with 3-hourly gauge data," J. Hydrometeorol, 2009, 10, pp. 149–166.

[25] Wolff, D. B., and co-authors, "Ground validation for the TRMM," J. Atmos. Oceanic Technol., 2005, 22, 365–380.

[26] Xie, P., and Arkin, P. A., "An intercomparison of gauge observations and satellite estimates of monthly precipitation," Journal of Applied Meteorology, 1995, 34, pp. 1143–1160.

[27] Krajewski, W. F., and co-authors., "Initial validation of the Global Precipitation Climatology Project monthly rainfall over the US," J. App. Met., 2000, 39, 1071–1086.

[28] Adler, R. F., and co-authors., "Intercomparison of global precipitation products: the Third Precipitation Intercomparison Project," Bulletin of the Amer. Meteo. Soc., 2001, 82, pp. 1377–1396.

[29] Gebremichael, M., et al., "A detailed evaluation of GPCP one-degree daily rainfall estimates over the Mississippi River Basin," Journal of Applied Meteorology, 2005, 44, pp. 665–681.

[30] Adler, R. F., and co-authors., "Status of TRMM monthly estimates of tropical precipitation, in Cloud Systems, Hurricanes, and the TRMM," Met. Soc. Monogr., 2003, 29, 223–234.

[31] Nicholson, S. E., et al., "Validation of TRMM and other rainfall estimates with a high-density gauge dataset for West Africa. Part I," J. Appl. Meteorol., 2003, 42, 1337–1354.

[32] Bookhagen, B., and Burbank, D. W., “Towards a complete Himalayan hydrological budget: The spatiotemporal distribution of snow melt and rainfall and their impact on river discharge,” J. Geophys. Research-Earth Surface, 2010, doi:10.1029/2009jf001426.

[33] Bookhagen, B., and Strecker, M. R., “Orographic barriers, high-resolution TRMM rainfall and relief variations along the eastern Andes,” Geophysical Research Letters, 2008, 35, L06403.

[34] Kunkel, K. E., and co-authors., “Temporal fluctuations in weather and climate extremes that cause economic and human health impacts,” B. Am. Meteor. Soc., 1999, 80:1077-1098.

[35] Ozcan, O., Bookhagen, B., and Musaoglu, N., “Impact of the Ataturk Dam Lake on Agro-Meteorological Aspects of the Southeastern Anatolia Region Using Remote Sensing and GIS Analysis,” XXII. ISPRS Congress, 2012, 25 Aug.-1 Sept., Melbourne.

[36] Hosking, J. R. M., and Wallis, J. R., “Regional Frequency Analysis, An Approach Based on Lmoments,” *Cambr. Univ. Pr.*, 1997.

[37] Cunnane, C., “Statistical Distributions for Flood Frequency Analysis.” Operational Hydrology Report no. 33, World Meteorological Organization, 1989.

[38] Gilli, M., and Kellezi, E., “An Application of Extreme Value Theory for Measuring Risk (Switzerland: Geneva),” 2003.